Original Research Article

An Immersed Finite Element Method for Planar Elasticity Interface Problem☆

Abstract

We present the P_1/CR immersed finite element (IFE) method to solve planar elasticity interface problem. By adding some stabilisation terms on the edges of interface elements, we show the stability of the discrete formulation and a priori error estimate in an energy norm. Finally, numerical examples are given to confirm our theoretical results.

Keywords: interface problem, IFE method, penalty terms

1. Introduction

Linear elasticity equation plays an important role in solid mechanics. In particular, problems involving composite materials are getting more attention from both engineers and mathematicians in recent years, for example, the atomic interactions [14] and the crystalline materials problems [37].

We consider a planar object made of two elastic materials and separated by a curve Γ in the bounded polygonal domain $\Omega \subseteq \mathbb{R}^2$, as illustrated in Fig. 1. The Lamé coefficients μ and λ are piecewise positive constants

$$(\mu, \lambda) = \begin{cases} (\mu^-, \lambda^-), & \text{in } \Omega^-, \\ (\mu^+, \lambda^+), & \text{in } \Omega^+, \end{cases}$$

which are defined by the Poisson ratio ν and the Young's module E as

$$\mu = \frac{E}{2(1+\nu)}, \qquad \lambda = \frac{E\nu}{(1+\nu)(1-2\nu)}.$$

The model problem is to find the displacement variable $\boldsymbol{u}$ such that

$$-\nabla \cdot \boldsymbol{\sigma}(\boldsymbol{u}) = \boldsymbol{f}, \quad \text{in } \Omega^- \cup \Omega^+, \tag{1.1}$$

$$\boldsymbol{u} = \boldsymbol{0}, \quad \text{on } \partial\Omega, \tag{1.2}$$

where the symmetric stress tensor

$$\boldsymbol{\sigma}(\boldsymbol{u}) = 2\mu\boldsymbol{\epsilon}(\boldsymbol{u}) + \lambda tr(\boldsymbol{\epsilon}(\boldsymbol{u}))\boldsymbol{I},$$

$\boldsymbol{\epsilon}(\boldsymbol{u}) = \frac{1}{2}(\nabla \boldsymbol{u} + (\nabla \boldsymbol{u})^t)$ is the strain tensor with the trace being $tr(\boldsymbol{\epsilon}) = \Sigma_{i=1}^{2} \epsilon_{ii}$, $\boldsymbol{I}$ is the identity matrix, and $\boldsymbol{f} \in (L^2(\Omega))^2$ is the external force. On the interface Γ, we assume that $\boldsymbol{u}$ satisfies the following interface conditions

$$[\boldsymbol{u}] = \boldsymbol{0}, \quad \text{on } \Gamma, \tag{1.3}$$

$$[\boldsymbol{\sigma}(\boldsymbol{u})\boldsymbol{n}] = \boldsymbol{0}, \quad \text{on } \Gamma, \tag{1.4}$$

where $\boldsymbol{n} = (n_1, n_2)^t$ is the unit outer normal vector of the interface pointing from Ω^+ to Ω^-.

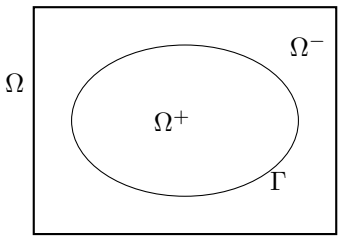

Fig. 1 A separated domain Ω.

In the last decades, a large number of numerical methods have been proposed for solving composite material problems. At the beginning, the interface-fitted mesh methods are widely used. But when we solve problems with complex interface, especially for moving interface problems, it is difficult and time consuming to generate an interface-fitted mesh. Consequently, the unfitted-mesh methods are put forward and developed, for instance, the extended finite element method [16, 35] and the immersed finite element (IFE) method [25, 27, 34, 28].

We focus on the IFE method, which have been developed in a series of significant interface problems. This method was first proposed by Li in [25] and applied by many authors in [1, 13, 19, 23, 38, 15, 32, 34, 29, 30, 20]. In [28], a partially penalized IFE method is applied to the second order elliptic equations and the optimal finite element error estimate is obtained in 2D case. In [34] and [33], two kinds of IFE methods are developed for the planar elasticity systems, which are based on rotated Q_1 elements and P_1/CR IFE elements respectively. But both of them only figure out the unisolvent property of the IFE space, there is no theoretical result for the approximation capability or any other further analysis. In [24], we present a P_1/CR IFE method with midpoint values on edges as degrees of freedom for CR elements and prove the approximation capability of our method. Furthermore, we give the error estimate of the IFE method in an energy norm.

In this article, to further perfect the P_1/CR IFE method, we use the integration average values on edges as degrees of freedom for CR elements to solve the planar elasticity interface problems. We give the proof of the approximation capability in L^2 norm and H^1 semi-norm. Because of the negative impacts from the discontinuity over edges, some penalty terms are added to enhance the stability so that the optimal error estimate of the new method has also been demonstrated.

The rest of this paper is organized as follow. Some notion and the partially penalized P_1/CR IFE method are given in next section. In Section 3, we present the important

trace inequality. The error estimate of the IFE method is derived in an energy norm in Section 4. Finally, some numerical examples are given.

2. The P_1/CR IFE method

Let $\mathcal{T}_h$ be a regular Cartesian triangular mesh of Ω. Let $\mathcal{T}_h^i = \{T \in \mathcal{T}_h;\ T \cap \Gamma \neq \emptyset\}$ and $\mathcal{T}_h^n = \mathcal{T}_h / \mathcal{T}_h^i$ represent the set of interface elements and the set of non-interface elements, respectively. Define the set of all sides $\varepsilon_h = \{e \subseteq \partial T;\ T \in \mathcal{T}_h\}$, the set of the non-cut edges $\varepsilon_h^n = \{e \subseteq \partial T;\ e \cap \Gamma = \emptyset,\ T \in \mathcal{T}_h\}$, the set of the cut edges $\varepsilon_h^i = \{e \subseteq \partial T;\ e \cap \Gamma \neq \emptyset,\ T \in \mathcal{T}_h^i\}$. We assume that interface elements satisfy the following assumptions when the mesh size h is small enough.

(**H1**) The interface Γ can't intersect the boundary of any element at more than two points unless one edge is part of Γ.

(**H2**) If Γ intersects the boundary of a element at two points, these intersection points must be on different edges of this element.

For every interior edge $e \in \varepsilon_h$, we assume that two elements $T_{e,1}$ and $T_{e,2}$ share the common edge e. For a function $\boldsymbol{u}$, define

$$\{\boldsymbol{u}\}_e = \frac{1}{2}\left((\boldsymbol{u}|_{T_{e,1}})|_e + (\boldsymbol{u}|_{T_{e,2}})\right)|_e, \quad [\boldsymbol{u}]_e = (\boldsymbol{u}|_{T_{e,1}})|_e - (\boldsymbol{u}|_{T_{e,2}})|_e.$$

For simplicity's sake, we will drop the subscript e from these notations. Denote the function space

$$(\widetilde{H}^2(\Omega))^2 = \left\{\boldsymbol{u} \in (H^1(\Omega))^2 : \boldsymbol{u}|_{\Omega^s} \in (H^2(\Omega^s))^2,\ s = +,\ -\right\},$$

which is equipped with the norm $\|\boldsymbol{u}\|_{\tilde{H}^2(\Omega)}$, where

$$\|\boldsymbol{u}\|^2_{\widetilde{H}^2(\Omega)} = \|\boldsymbol{u}\|^2_{H^1(\Omega)} + \|\boldsymbol{u}\|^2_{H^2(\Omega^-)} + \|\boldsymbol{u}\|^2_{H^2(\Omega^+)}.$$

Multiplying $\boldsymbol{v} \in (H_0^1(\Omega))^2$ to the both sides of (1.1) and applying Greens formula in each domain Ω^s $(s = +, -)$, we deduce that

$$\int_{\Omega^s} \boldsymbol{\sigma}(\boldsymbol{u}) : \boldsymbol{\epsilon}(\boldsymbol{v}) d\boldsymbol{x} - \int_{\Omega^s} \boldsymbol{\sigma}(\boldsymbol{u})\boldsymbol{n} \cdot \boldsymbol{v} ds = \int_{\Omega^s} \boldsymbol{f} \cdot \boldsymbol{v} d\boldsymbol{x}.$$

Summing over $s = +, -$, we obtain the following weak form: finding $\boldsymbol{u} \in V = \left\{\boldsymbol{\omega} \in (H^1(\Omega))^2 \middle|\ \boldsymbol{\omega}|_{\partial\Omega} = \boldsymbol{g}\right\}$ such that

$$a(\boldsymbol{u}, \boldsymbol{v}) = (\boldsymbol{f}, \boldsymbol{v}), \quad \forall \boldsymbol{v} \in (H_0^1(\Omega))^2, \tag{2.5}$$

where

$$a(\boldsymbol{u}, \boldsymbol{v}) = \int_\Omega \boldsymbol{\sigma}(\boldsymbol{u}) : \boldsymbol{\epsilon}(\boldsymbol{v}) d\boldsymbol{x},$$

and

$$(\boldsymbol{f}, \boldsymbol{v}) = \int_\Omega \boldsymbol{f} \cdot \boldsymbol{v} d\boldsymbol{x}.$$

Now, we give the P_1/CR IFE method, which has been proposed in [33]. For completeness, we descript it simply.

In the non-interface element T, we apply the standard P_1/CR finite element space $S_h^n(T) = \text{Span}\{\boldsymbol{\psi}_{j,T} : j = 1, 2, \cdots, 6\}$. The local basis functions are chosen to satisfy the following conditions

$$\boldsymbol{\psi}_{j,T}(A_i) = \begin{pmatrix} \delta_{i,j} \\ 0 \end{pmatrix}, \qquad j = 1, 2, 3; \tag{2.6}$$

and

$$\frac{1}{|e_i|}\int_{e_i} \boldsymbol{\psi}_{j,T} ds = \begin{pmatrix} 0 \\ \delta_{j-3,i} \end{pmatrix}, \qquad j = 4, 5, 6, \tag{2.7}$$

where A_i and B_i (i=1, 2, 3) are the vertices and the edges of T respectively, and δ_{ij} is the Kronecker symbol.

For the interface element T, let $D = (x_D, y_D)$, $E = (x_E, y_E)$ be the intersections of the interface with T, the line segment $\overline{DE}$ separates element into two subelements T^+ and T^-. We use $\overline{DE}$ to approximate the curve $\widetilde{DE} = \Gamma \cap T$ so that the interface is perturbed by an $O(h^2)$ term. We only describe the basis functions on the reference interface element $\hat{T} =\triangle\, \hat{A}_1\hat{A}_2\hat{A}_3$, where $\hat{A}_1 = (0, 0),\ \hat{A}_2 = (1, 0),\ \hat{A}_3 = (0, 1)$.

Suppose that $\hat{D} = (\hat{d}, 0)$ and $\hat{E} = (0, \hat{e})$, $0 < \hat{d}, \hat{e} < 1$. The piecewise linear P_1/CR IFE function on $\hat{T}$ is

$$\hat{\boldsymbol{\phi}}_j = \begin{cases} \hat{\phi}_{1,j} = \begin{pmatrix} \hat{\phi}^+_{1,j} \\ \hat{\phi}^-_{1,j} \end{pmatrix} = \begin{pmatrix} a_1^+ + b_1^+\hat{x} + c_1^+\hat{y} \\ a_1^- + b_1^-\hat{x} + c_1^-\hat{y} \end{pmatrix} & \begin{matrix} \text{if } (\hat{x}, \hat{y}) \in \hat{T}^+, \\ \text{if } (\hat{x}, \hat{y}) \in \hat{T}^-, \end{matrix} \\ \hat{\phi}_{2,j} = \begin{pmatrix} \hat{\phi}^+_{2,j} \\ \hat{\phi}^-_{2,j} \end{pmatrix} = \begin{pmatrix} a_2^+ + b_2^+\hat{x} + c_2^+\hat{y} \\ a_2^- + b_2^-\hat{x} + c_2^-\hat{y} \end{pmatrix} & \begin{matrix} \text{if } (\hat{x}, \hat{y}) \in \hat{T}^+, \\ \text{if } (\hat{x}, \hat{y}) \in \hat{T}^-, \end{matrix} \end{cases} \tag{2.8}$$

where, a_i^s, b_i^s, c_i^s ($i = 1,\ 2$ and $s = +, -$) are undetermined coefficients. We can determine the basis function $\hat{\boldsymbol{\phi}}_j$ ($j = 1, 2, \cdots, 6$) by the following conditions, the values at the vertices

$$\hat{\phi}_{1,j}(\hat{A}_i) = \delta_{ij}, \qquad i = 1, 2, 3, \tag{2.9}$$

the integral average values at the edges of $\hat{T}$

$$\frac{1}{|\hat{e}_i|}\int_{\hat{e}_i} \hat{\phi}_{2,j} ds = \delta_{i,j-3}, \qquad i = 1, 2, 3, \tag{2.10}$$

the continuity of displacement at the intersection points ($i = 1,\ 2$)

$$\hat{\phi}^+_{i,j}(\hat{D}) = \hat{\phi}^-_{i,j}(\hat{D}), \qquad \hat{\phi}^+_{i,j}(\hat{E}) = \hat{\phi}^-_{i,j}(\hat{E}), \tag{2.11}$$

the traction continuity along the interface

$$\begin{cases} \left[(\lambda + 2\mu)\frac{\partial \hat{\phi}_{1,j}}{\partial x}\bar{n}_1 + \lambda\frac{\partial \hat{\phi}_{2,j}}{\partial y}\bar{n}_1 + \mu\left(\frac{\partial \hat{\phi}_{1,j}}{\partial y} + \frac{\partial \hat{\phi}_{2,j}}{\partial x}\right)\bar{n}_2\right]\Big|_{\overline{\hat{D}\hat{E}}} = 0, \\ \left[\mu\left(\frac{\partial \hat{\phi}_{1,j}}{\partial y} + \frac{\partial \hat{\phi}_{2,j}}{\partial x}\right)\bar{n}_1 + \lambda\frac{\partial \hat{\phi}_{1,j}}{\partial x}\bar{n}_2 + (\lambda + 2\mu)\frac{\partial \hat{\phi}_{2,j}}{\partial y}\bar{n}_2\right]\Big|_{\overline{\hat{D}\hat{E}}} = 0, \end{cases} \tag{2.12}$$

where $\bar{\boldsymbol{n}} = (\bar{n}_1, \bar{n}_2)$ is the unit outer normal to the segment $\overline{DE}$.

The unisolvent property of this method has been proved in [33]. Define the local basis functions $\boldsymbol{\phi}_j$ on the element T as $\boldsymbol{\phi}_{j,T}$, the local P_1/CR IFE space $S_h^i(T)$ is given by

$$S_h^i(T) = \text{Span}\{\boldsymbol{\phi}_{j,T} : j = 1, 2, \cdots, 6\}.$$

The global P_1/CR IFE space can be expressed as

$$S_h(\Omega) = \big\{\boldsymbol{v}_h = (v_{1h}, v_{2h})^t \in (L^2(\Omega))^2 : \boldsymbol{v}_h|_T \in S_h^\alpha(T),\ \alpha = i, n,\ \forall T \in \mathcal{T}_h;$$
$$\boldsymbol{v}_{1h}|_{T_1}(A_j) = \boldsymbol{v}_{1h}|_{T_2}(A_j),\ j = 1, 2,\ \text{and}\ \int_{\overline{A_1A_2}} \boldsymbol{v}_{2h}|_{T_1} ds = \int_{\overline{A_1A_2}} \boldsymbol{v}_{2h}|_{T_2} ds,$$
$$\forall T_1 \cap T_2 = \overline{A_1A_2}\big\}.$$

Define the energy norm

$$\|\boldsymbol{v}_h\|_h = \left(\sum_{T\in\mathcal{T}_h} \big(\boldsymbol{\sigma}(\boldsymbol{v}_h), \boldsymbol{\epsilon}(\boldsymbol{v}_h)\big)_T + \sum_{e\in\varepsilon_h^i} h^{-1}(\mu+\lambda)([\boldsymbol{v}_h], [\boldsymbol{v}_h])_e \right)^{\frac{1}{2}}. \tag{2.13}$$

The discrete problem for the planar elasticity interface problem reads as: to find $\boldsymbol{u}_h \in S_h(\Omega)$ such that

$$a_h(\boldsymbol{u}_h, \boldsymbol{v}_h) = (\boldsymbol{f}, \boldsymbol{v}_h), \quad \forall \boldsymbol{v}_h \in S_{h,0}(\Omega), \tag{2.14}$$

where

$$S_{h,0}(\Omega) = \big\{\boldsymbol{v}_h = (v_{1,h}, v_{2,h})^t \in S_h(\Omega),\ \text{if}\ \partial T \cap \partial\Omega = \overline{A_1A_2},\ v_{1,h}|(A_i) = g_1(A_i),\ i = 1,\ 2,$$
$$\text{and}\ \int_{\overline{A_1A_2}} v_{2,h} ds = \int_{\overline{A_1A_2}} v_{2,h} ds = 0,\ T \in \mathcal{T}_h\big\},$$

$$a_h(\boldsymbol{u}_h, \boldsymbol{v}_h) = \sum_{T\in\mathcal{T}_h} \big(\boldsymbol{\sigma}(\boldsymbol{u}_h), \boldsymbol{\epsilon}(\boldsymbol{v}_h)\big)_T - \sum_{e\in\varepsilon_h^i} \big(\{\boldsymbol{\sigma}(\boldsymbol{u}_h)\cdot\mathbf{n}\}, [\boldsymbol{v}_h]\big)_e$$
$$- \sum_{e\in\varepsilon_h^i} \big(\{\boldsymbol{\sigma}(\boldsymbol{v}_h)\cdot\mathbf{n}\}, [\boldsymbol{u}_h]\big)_e + \sum_{e\in\varepsilon_h^i} h^{-1}(\mu+\lambda)([\boldsymbol{u}_h], [\boldsymbol{v}_h])_e,$$

and

$$(\boldsymbol{f}, \boldsymbol{v}_h) = \int_\Omega \boldsymbol{f}\cdot\boldsymbol{v}_h d\boldsymbol{x}.$$

3. Bounds for the interpolation error

For any interface triangle $T \in \mathcal{T}_h$, let

$$(\widetilde{H}^2(T))^2 = \big\{\boldsymbol{u} \in (H^1(T))^2,\ \boldsymbol{u}|_{T^s} \in (H^2(T^s))^2,\ s = +, -,\ [\boldsymbol{\sigma}(\boldsymbol{u})\boldsymbol{n}] = \mathbf{0}\ \text{on}\ \Gamma\cap T\big\}.$$

By the Theorem 4.10 in [24], the following lemma holds.

Lemma 3.1. *For any $\boldsymbol{u} \in (\widetilde{H}^2(\Omega))^2$, there exists constants $C > 0$ such that*

$$\big\|I_{h,T}^p\boldsymbol{u} - \boldsymbol{u}\big\|_{0,T} + h\big|I_{h,T}^p\boldsymbol{u} - \boldsymbol{u}\big|_{1,T} \le Ch^2\|\boldsymbol{u}\|_{\widetilde{H}^2(T)}, \tag{3.15}$$
$$\|I_h^p\boldsymbol{u} - \boldsymbol{u}\|_{0,\Omega} + h\,|I_h^p\boldsymbol{u} - \boldsymbol{u}|_{1,\Omega} \le Ch^2\|\boldsymbol{u}\|_{\widetilde{H}^2(\Omega)}, \tag{3.16}$$

where $I_{h,T}^p$ and I_h^p are the corresponding local IFE and global IFE interpolation operators in [24], respectively.

Define a local interpolation operator $I_{h,T} : (\tilde{H}^2(T))^2 \to S_h(T)$ as

$$I_{h,T}\boldsymbol{u} = \begin{cases} \sum_{j=1}^{6} c_j \boldsymbol{\psi}_{j,T}, & \text{if } T \text{ is a non-interface element,} \\ \sum_{j=1}^{6} c_j \boldsymbol{\phi}_{j,T}, & \text{if } T \text{ is an interface element,} \end{cases}$$

where

$$c_i = u_1(A_i), \quad i = 1, 2, 3; \qquad c_j = \frac{1}{|e_{j-3}|} \int_{e_{j-3}} u_2 ds, \quad j = 4, 5, 6.$$

The global IFE interpolation operator $I_h : (\tilde{H}^2(\Omega))^2 \to S_h(\Omega)$ is denoted by

$$I_h\boldsymbol{u}|_T = I_{h,T}\boldsymbol{u}, \qquad \forall T \in \mathcal{T}_h.$$

At first, we give an error bound for IFE basis function $\phi_{i,T}$.

Lemma 3.2. *There exists a constant $C > 0$ such that*

$$\|\phi_{i,T}\|_{0,T} + h\,|\phi_{i,T}|_{1,T} \le Ch, \quad i = 1, \cdots, 6, \quad \forall T \in \mathcal{T}_h^i. \tag{3.17}$$

Proof. According to Theorem 2.4 in [26] and Theorem 3.2 in [39], the following estimate holds

$$\|\phi_{i,T}\|_{0,T}^2 = \int_T \phi_{i,T}^2(x,y)dxdy \le \|\phi_{i,T}\|_{0,\infty,T}^2 \int_T 1 dxdy \le Ch^2. \tag{3.18}$$

Similarly,

$$|\phi_{i,T}|_{1,T}^2 = \int_T \nabla\phi_{i,T}(x,y) \cdot \nabla\phi_{i,T}(x,y)dxdy \le |\phi_{i,T}|_{1,\infty,T}^2 \int_T 1 dxdy \le C. \tag{3.19}$$

Combining with (3.18) and (3.19), the desired result is obtained. □

Then we estimate the interpolation error $\boldsymbol{u} - I_{h,T}\boldsymbol{u}$.

Theorem 3.3. *There exists a constant $C > 0$ such that*

$$\|I_{h,T}\boldsymbol{u} - \boldsymbol{u}\|_{0,T} + h\,|I_{h,T}\boldsymbol{u} - \boldsymbol{u}|_{1,T} \le Ch^2\|\boldsymbol{u}\|_{2,T}, \quad \forall \boldsymbol{u} \in (\widetilde{H}^2(T))^2, \tag{3.20}$$

where $T \in \mathcal{T}_h^i$ is an arbitrary interface element.

Proof. By triangular inequality,

$$|I_{h,T}\boldsymbol{u} - \boldsymbol{u}|_{k,T} \le |I_{h,T}\boldsymbol{u} - I_{h,T}^p\boldsymbol{u}|_{k,T} + |I_{h,T}^p\boldsymbol{u} - \boldsymbol{u}|_{k,T}, \quad k = 0, 1, \tag{3.21}$$

where the notation $|\cdot|_{0,T}$ means the L^2 norm on T. The estimate of the term $|I_{h,T}^p\boldsymbol{u} - \boldsymbol{u}|_{k,T}$ can be obtained by Lemma 3.1. Hence, we only need to bound $|I_{h,T}\boldsymbol{u} - I_{h,T}^p\boldsymbol{u}|_{k,T}$. Let

$$\bar{\boldsymbol{u}}_i(X) = \frac{1}{|e_i|} \int_{e_i} \boldsymbol{u}(X) ds, \quad i = 1, 2, 3,$$

where e_i (i=1, 2, 3) is the edge of T. Then

$$\begin{aligned}
&I_{h,T}\boldsymbol{u}(X) - I^p_{h,T}\boldsymbol{u}(X)\\
&= \sum_{i=1}^{3} \boldsymbol{u}(A_i)(\boldsymbol{\phi}_i(X) - \boldsymbol{\phi}^p_i(X)) + \sum_{i=4}^{6} \boldsymbol{\phi}_{i-3}(X)\bar{\boldsymbol{u}}_{i-3}(X) - \sum_{i=4}^{6} \boldsymbol{\phi}^p_i(X)\boldsymbol{u}(M_{i-3})\\
&= \sum_{i=1}^{3} \boldsymbol{u}(A_i)(\boldsymbol{\phi}_i(X) - \boldsymbol{\phi}^p_i(X)) + \sum_{i=4}^{6} \bar{\boldsymbol{u}}_{i-3}(X)\,(\boldsymbol{\phi}_i(X) - \boldsymbol{\phi}^p_i(X))\\
&\quad + \sum_{i=4}^{6} \boldsymbol{\phi}^p_i(X)\,(\bar{\boldsymbol{u}}_{i-3}(X) - \boldsymbol{u}(M_{i-3}))\,,
\end{aligned} \tag{3.22}$$

where M_j ($j = 1,\ 2,\ 3$) is the midpoint of T and $\boldsymbol{\phi}^p_i(X)$ ($i = 1, \cdots, 6$) is the corresponding basis function on $T \in \mathcal{T}^i_h$ in [24]. We note that

$$\boldsymbol{\phi}_1 = \boldsymbol{\phi}^p_1 = (a^-_1,\ 0)^t,\quad \boldsymbol{\phi}_2 = \boldsymbol{\phi}^p_2 = (a^+_1 + b^+_1,\ 0)^t,\quad \boldsymbol{\phi}_3 = \boldsymbol{\phi}^p_3 = (a^+_1 + c^+_1,\ 0)^t, \tag{3.23}$$

and

$$\boldsymbol{\phi}_4 = (0,\ a^+_2 + \frac{1}{2}b^+_2)^t,\quad \boldsymbol{\phi}^p_4 = (0,\ a^-_2\, d + \frac{1}{2}b^-_2\, d^2 + a^+_2(1-d) + \frac{1}{2}b^+_2(1-d^2))^t, \tag{3.24}$$

$$\boldsymbol{\phi}_5 = (0,\ a^+_2 + \frac{1}{2}b^+_2 + \frac{1}{2}c^+_2)^t,\quad \boldsymbol{\phi}^p_5 = (0,\ a^+_2 + \frac{1}{2}b^+_2 + \frac{1}{2}c^+_2)^t, \tag{3.25}$$

$$\boldsymbol{\phi}_6 = (0,\ a^-_2 + \frac{1}{2}c^-_2)^t,\quad \boldsymbol{\phi}^p_6 = (0,\ a^-_2\, e + \frac{1}{2}c^-_2\, e^2 + a^+_2(1-e) + \frac{1}{2}c^+_2(1-e^2))^t. \tag{3.26}$$

Inserting the expressions (3.23)-(3.26) into (3.22) and integrating on T, we obtain

$$\begin{aligned}
&\|I_{h,T}\boldsymbol{u}(X) - I^p_{h,T}\boldsymbol{u}(X)\|_{k,T}\\
&= \left\| \sum_{i=4}^{6} [\bar{\boldsymbol{u}}_{i-3}(X)\,(\phi_i(X) - \phi^p_i(X)) + (\bar{\boldsymbol{u}}_{i-3}(X) - \boldsymbol{u}(M_{i-3}))\phi^p_i(X)] \right\|_{k,T}\\
&= \|I_1 + I_2\|_{k,T}\,.
\end{aligned}$$

Moreover, by Cacuchy-Schwarz inequality and Lemma 3.2,

$$\begin{aligned}
\|I_1\|_{k,T} &\le \sum_{i=4}^{6} \frac{1}{|e_{i-3}|^{1/2}} \|\boldsymbol{u}\|_{0,e_{i-3}} \|\phi_i(X) - \phi^p_i(X)\|_{k,T}\\
&\le Ch^{1-k} \sum_{i=4}^{6} \frac{1}{|e_{i-3}|^{1/2}} (h^{-1/2}\|\boldsymbol{u}\|_{0,T} + h^{1/2}|\boldsymbol{u}|_{1,T})\\
&\le C(h^{-k}\|\boldsymbol{u}\|_{0,T} + h^{1-k}|\boldsymbol{u}|_{1,T}).
\end{aligned} \tag{3.27}$$

According to the Taylor expansion and Lemma 3.2 in [24], we deduce that

$$\begin{aligned}\|I_2\|_{k,T} &\le C\sum_{i=1}^{3}\frac{1}{|e_i|}\int_{e_i}|\nabla \boldsymbol{u}(X)(X-M_i)|ds\\ &\le Ch\sum_{i=1}^{3}\frac{1}{|e_i|^{1/2}}\|\nabla \boldsymbol{u}(X)\|_{0,e_i}\\ &\le Ch\sum_{i=1}^{3}\frac{1}{|e_i|^{1/2}}(h^{-1/2}\|\nabla \boldsymbol{u}\|_{0,T}+h^{1/2}|\nabla \boldsymbol{u}|_{1,T})\\ &\le C(\|\boldsymbol{u}\|_{1,T}+h|\boldsymbol{u}|_{2,T}).\end{aligned} \tag{3.28}$$

Combining (3.27) with (3.28),

$$|I_{h,T}\boldsymbol{u}-I^{p}_{h,T}\boldsymbol{u}|_{k,T}\le C(h^{-k}h^2\|\boldsymbol{u}\|_{2,T}+h^{1-k}h\|\boldsymbol{u}\|_{2,T})\le Ch^{2-k}\|\boldsymbol{u}\|_{2,T}. \tag{3.29}$$

The proof is completed. □

Summing over all the elements, the following estimate holds.

Theorem 3.4. *There exists a constant C such that*

$$\|I_{h,T}\boldsymbol{u}-\boldsymbol{u}\|_{0,\Omega}+h|I_{h,T}\boldsymbol{u}-\boldsymbol{u}|_{1,\Omega}\le Ch^2\|\boldsymbol{u}\|_{\widetilde{H}^2(\Omega)},\quad \forall \boldsymbol{u}\in(\widetilde{H}^2(\Omega))^2. \tag{3.30}$$

At last, we give the estimate of interpolation error in the energy norm.

Theorem 3.5. *There exists a constant $C>0$, such that*

$$\|\boldsymbol{u}-I_h\boldsymbol{u}\|_h\le Ch\|\boldsymbol{u}\|_{\widetilde{H}^2(\Omega)},\quad \forall \boldsymbol{u}\in(\widetilde{H}^2(\Omega))^2. \tag{3.31}$$

Proof. Taking (2.13) into consideration, we get

$$\begin{aligned}\|\boldsymbol{u}-I_h\boldsymbol{u}\|_h^2=&\sum_{T\in\mathcal{T}_h}\big(\boldsymbol{\sigma}(\boldsymbol{u}-I_h\boldsymbol{u}),\boldsymbol{\epsilon}(\boldsymbol{u}-I_h\boldsymbol{u})\big)_T\\ &+\sum_{e\in\varepsilon_h^i}h^{-1}(\mu+\lambda)([\boldsymbol{u}-I_h\boldsymbol{u}],[\boldsymbol{u}-I_h\boldsymbol{u}])_e,\end{aligned} \tag{3.32}$$

According to Theorem 3.4,

$$\sum_{T\in\mathcal{T}_h}\big(\boldsymbol{\sigma}(\boldsymbol{u}-I_h\boldsymbol{u}),\boldsymbol{\epsilon}(\boldsymbol{u}-I_h\boldsymbol{u})\big)_T\le Ch^2\|\boldsymbol{u}\|^2_{\widetilde{H}^2(\Omega)}. \tag{3.33}$$

By the standard trace inequality, the last term in (3.32) can be deduced that

$$\begin{aligned}\|[\boldsymbol{u}-I_h\boldsymbol{u}]\|^2_{0,e}&\le(\|(\boldsymbol{u}-I_h\boldsymbol{u})|_{T_1}\|_{0,e}+\|(\boldsymbol{u}-I_h\boldsymbol{u})|_{T_2}\|_{0,e})^2\\ &\le\sum_{i=1}^{2}C|e||T_i|^{-1}(\|(\boldsymbol{u}-I_h\boldsymbol{u})\|_{0,T_i}+h\|\nabla(\boldsymbol{u}-I_h\boldsymbol{u})\|_{0,T_i})^2\\ &\le\sum_{i=1}^{2}C|e|(h\|\boldsymbol{u}\|_{\widetilde{H}^2(T_i)})^2.\end{aligned} \tag{3.34}$$

Combining (3.34) with (3.32) and (3.33), the desired result is obtained. □

4. The error estimates

We start by giving the trace inequality of the IFE functions in $S_h^i(T)$ for $T \in \mathcal{T}_h^i$. By the similar techniques of Lemma 5.1 and Lemma 5.2 in [24], we have the following lemmas.

Lemma 4.1. *For any IFE function $\boldsymbol{v} \in S_h^i(T)$ defined as (2.8), there exists a constant C such that*

$$\frac{1}{C}\|(b_1^+, c_1^+, b_2^+, c_2^+)\| \leq \|(b_1^-, c_1^-, b_2^-, c_2^-)\| \leq C\|(b_1^+, c_1^+, b_2^+, c_2^+)\|, \tag{4.35}$$

where $\|\cdot\|$ is a Euclidean norm.

Lemma 4.2. *For an arbitrary IFE function $\boldsymbol{v}$, there exists a constant C such that*

$$\|\mu\boldsymbol{\epsilon}(\boldsymbol{v})\cdot\mathbf{n}\|_{0,e} \leq Ch^{1/2}|T|^{1/2}\|\mu\boldsymbol{\epsilon}(\boldsymbol{v})\|_{0,T}, \tag{4.36}$$

$$\|\lambda(\nabla\cdot\boldsymbol{v})I\cdot\mathbf{n}\|_{0,e} \leq Ch^{1/2}|T|^{1/2}\|\mu\boldsymbol{\epsilon}(\boldsymbol{v})\|_{0,T}, \tag{4.37}$$

where $T \in \mathcal{T}_h^i$ is an interface element.

Now, we have the following trace inequality.

Lemma 4.3. *There exists a constant C such that the following inequality holds*

$$\sum_{e\in\varepsilon_h^i}\left(h\{\boldsymbol{n}\cdot\boldsymbol{\sigma}(\boldsymbol{v})\},\{\boldsymbol{n}\cdot\boldsymbol{\epsilon}(\boldsymbol{v})\}\right)_e \leq C\sum_{T\in\mathcal{T}_h^i}(\boldsymbol{\sigma}(\boldsymbol{v}),\boldsymbol{\epsilon}(\boldsymbol{v}))_T, \qquad \forall\boldsymbol{v}\in S_h(\Omega). \tag{4.38}$$

Proof. For any interface edge $e = T_1 \cap T_2$, we first note that

$$\begin{aligned}\left(h\boldsymbol{n}\cdot\boldsymbol{\sigma}(\boldsymbol{v}),\boldsymbol{n}\cdot\boldsymbol{\epsilon}(\boldsymbol{v})\right)_e &= h\left(\boldsymbol{n}\cdot(2\mu\boldsymbol{\epsilon}(\boldsymbol{v})+\lambda(\nabla\cdot\boldsymbol{v})I),\boldsymbol{n}\cdot\boldsymbol{\epsilon}(\boldsymbol{v})\right)_e\\ &= h\|\lambda(\nabla\cdot\boldsymbol{v})I\cdot\boldsymbol{n}\|_{0,e}^2 + 2h\|\mu\boldsymbol{\epsilon}(\boldsymbol{v})\cdot\boldsymbol{n}\|_{0,e}^2.\end{aligned} \tag{4.39}$$

Combining (4.40) with (4.36) and (4.37),

$$\begin{aligned}&\left(h\{\boldsymbol{n}\cdot\boldsymbol{\sigma}(\boldsymbol{v})\},\{\boldsymbol{n}\cdot\boldsymbol{\epsilon}(\boldsymbol{v})\}\right)_e\\ &\leq \frac{1}{2}\left((h\boldsymbol{n}\cdot\boldsymbol{\sigma}(\boldsymbol{v})|_{T_1},\boldsymbol{n}\cdot\boldsymbol{\epsilon}(\boldsymbol{v})|_{T_1})_e + (h\boldsymbol{n}\cdot\boldsymbol{\sigma}(\boldsymbol{v})|_{T_2},\boldsymbol{n}\cdot\boldsymbol{\epsilon}(\boldsymbol{v})|_{T_2})_e\right)\\ &\leq C\left(\|\mu\boldsymbol{\epsilon}(\boldsymbol{v})\cdot\boldsymbol{n}\|_{0,T_1}^2 + \|\mu\boldsymbol{\epsilon}(\boldsymbol{v})\cdot\boldsymbol{n}\|_{0,T_2}^2\right)\\ &\leq C\left((\boldsymbol{\sigma}(\boldsymbol{v}),\boldsymbol{\epsilon}(\boldsymbol{v}))_{T_1} + (\boldsymbol{\sigma}(\boldsymbol{v}),\boldsymbol{\epsilon}(\boldsymbol{v}))_{T_2}\right).\end{aligned}$$

Summing over all edges $e \in \varepsilon_h^i$, the proof is completed. □

Now we prove the coercivity of the bilinear form $a_h(\boldsymbol{u}_h,\boldsymbol{v}_h)$ in the IFE space.

Theorem 4.4. *There exists a constant $\kappa > 0$ such that*

$$\kappa\|\boldsymbol{v}_h\|_h^2 \leq a_h(\boldsymbol{v}_h,\boldsymbol{v}_h) \quad \forall\boldsymbol{v}_h\in S_{h,0}(\Omega). \tag{4.40}$$

Proof. Take consideration of (1.1), we deduce that

$$\boldsymbol{\epsilon} = \frac{1}{2\mu}(\boldsymbol{\sigma} - \frac{\lambda}{2\mu + 2\lambda} tr\boldsymbol{\sigma} I) = \frac{1}{2\mu}\boldsymbol{\sigma}^D + \frac{1}{4(\mu+\lambda)} tr\boldsymbol{\sigma} I,$$

where $\boldsymbol{\sigma}^D = \boldsymbol{\sigma} - (tr\boldsymbol{\sigma} I)/2$. Furthermore,

$$\begin{aligned}
\boldsymbol{\sigma} : \boldsymbol{\epsilon} &= \frac{1}{2\mu}\boldsymbol{\sigma}^D : \boldsymbol{\sigma}^D + \frac{1}{4(\mu+\lambda)}(tr\boldsymbol{\sigma})^2, \\
\boldsymbol{\sigma} : \boldsymbol{\sigma} &= \boldsymbol{\sigma}^D : \boldsymbol{\sigma}^D + \frac{1}{2}(tr\boldsymbol{\sigma})^2.
\end{aligned}$$

Thus $\boldsymbol{\sigma} : \boldsymbol{\sigma} = 2(\mu+\lambda)\boldsymbol{\sigma} : \boldsymbol{\epsilon}$, moreover,

$$\frac{1}{2}\left\| \frac{1}{\sqrt{\mu+\lambda}} \boldsymbol{n} \cdot \boldsymbol{\sigma}(\boldsymbol{v}_h) \right\|_{0,e}^2 \leq (\boldsymbol{n} \cdot \boldsymbol{\sigma}(\boldsymbol{v}_h), \boldsymbol{n} \cdot \boldsymbol{\epsilon}(\boldsymbol{v}_h))_e. \tag{4.41}$$

For each $e \in \varepsilon_h^i$, by using (4.41) and Cauchy-Schwarz inequality, there exists a constant $\delta > 0$ such that

$$\begin{aligned}
2(\boldsymbol{n} \cdot \boldsymbol{\sigma}(\boldsymbol{v}_h), [\boldsymbol{v}_h])_e &\leq 2\|\boldsymbol{n} \cdot \boldsymbol{\sigma}(\boldsymbol{v}_h)\|_{0,e} \|[\boldsymbol{v}_h]\|_{0,e} \\
&\leq \delta h \left\| \frac{1}{\sqrt{\mu+\lambda}} \boldsymbol{n} \cdot \boldsymbol{\sigma}(\boldsymbol{v}_h) \right\|_{0,e}^2 + \frac{4}{\delta h} \left\| \sqrt{\mu+\lambda}[\boldsymbol{v}_h] \right\|_{0,e}^2 \\
&\leq 2\delta h \left(\boldsymbol{n} \cdot \boldsymbol{\sigma}(\boldsymbol{v}_h), \boldsymbol{n} \cdot \boldsymbol{\epsilon}(\boldsymbol{v}_h)\right)_e + \frac{4}{\delta h} \left\| \sqrt{\mu+\lambda}[\boldsymbol{v}_h] \right\|_{0,e}^2 .
\end{aligned} \tag{4.42}$$

Combining (4.42) with Lemma 4.3, we obtain

$$\begin{aligned}
&2 \sum_{e \in \varepsilon_h^i} (\{\boldsymbol{n} \cdot \boldsymbol{\sigma}(\boldsymbol{v}_h)\}, [\boldsymbol{v}_h])_e \\
&\leq \sum_{e \in \varepsilon_h^i} 2\delta h \left(\boldsymbol{n} \cdot \boldsymbol{\sigma}(\boldsymbol{v}_h), \boldsymbol{n} \cdot \boldsymbol{\epsilon}(\boldsymbol{v}_h)\right)_e + \sum_{e \in \varepsilon_h^i} \frac{4}{\delta h} \left\| \sqrt{\mu+\lambda}[\boldsymbol{v}_h] \right\|_{0,e}^2 \\
&\leq \sum_{T \in \mathcal{T}_h^i} C\delta \left(\boldsymbol{\sigma}(\boldsymbol{v}_h), \boldsymbol{\epsilon}(\boldsymbol{v}_h)\right)_e + \sum_{e \in \varepsilon_h^i} \frac{4}{\delta h} ((\mu+\lambda)[\boldsymbol{v}_h], [\boldsymbol{v}_h])_e.
\end{aligned}$$

Finally,

$$\begin{aligned}
a_h(\boldsymbol{v}_h, \boldsymbol{v}_h) &= \sum_{T \in \mathcal{T}_h} \left(\boldsymbol{\sigma}(\boldsymbol{v}_h), \boldsymbol{\epsilon}(\boldsymbol{v}_h)\right)_T - 2 \sum_{e \in \varepsilon_h^i} \left(\{\boldsymbol{\sigma}(\boldsymbol{v}_h) \cdot \boldsymbol{n}\}, [\boldsymbol{v}_h]\right)_e \\
&\quad + \sum_{e \in \varepsilon_h^i} h^{-1} ((\mu+\lambda)[\boldsymbol{v}_h], [\boldsymbol{v}_h])_e \\
&\geq \sum_{T \in \mathcal{T}_h} \left(\boldsymbol{\sigma}(\boldsymbol{v}_h), \boldsymbol{\epsilon}(\boldsymbol{v}_h)\right)_T - 2 \sum_{T \in \mathcal{T}_h^i} C\delta \left(\boldsymbol{\sigma}(\boldsymbol{v}_h), \boldsymbol{\epsilon}(\boldsymbol{v}_h)\right)_e \\
&\quad - 2 \sum_{e \in \varepsilon_h^i} \frac{4}{\delta h} ((\mu+\lambda)[\boldsymbol{v}_h], [\boldsymbol{v}_h])_e + \sum_{e \in \varepsilon_h^i} h^{-1} ((\mu+\lambda)[\boldsymbol{v}_h], [\boldsymbol{v}_h])_e
\end{aligned}$$

Therefore, there exists a κ such that $a_h(\boldsymbol{v}_h, \boldsymbol{v}_h) \geq \kappa \|\boldsymbol{v}_h\|_h^2$ with a proper δ. □

Theorem 4.5. *Let $\boldsymbol{u} \in (\widetilde{H}^2(\Omega))^2$ and $\boldsymbol{u}_h \in S_h(\Omega)$ are the solutions of (2.5) and (2.14), respectively. Then there exists a constant C such that*

$$\|\boldsymbol{u} - \boldsymbol{u}_h\|_h \leq Ch\|\boldsymbol{u}\|_{\widetilde{H}^2(\Omega)}. \tag{4.43}$$

Proof. By the second Strang lemma, we note that

$$\|\boldsymbol{u} - \boldsymbol{u}_h\|_h \leq C\left(\inf_{\forall \boldsymbol{v}_h \in S_{h,0}(\Omega)} \|\boldsymbol{u} - \boldsymbol{v}_h\|_h + \sup_{\forall \boldsymbol{w}_h \in S_{h,0}(\Omega)} \frac{|a_h(\boldsymbol{u}, \boldsymbol{w}_h) - (\boldsymbol{f}, \boldsymbol{w}_h)|}{\|\boldsymbol{w}_h\|_h}\right). \tag{4.44}$$

By the Cauchy-Schwarz inequality and the standard trace theorem, the last term in (4.44) can be deduced that

$$\begin{aligned} |a_h(\boldsymbol{u}, \boldsymbol{w}_h) - (\boldsymbol{f}, \boldsymbol{w}_h)| &= \Big| \sum_{e \in \varepsilon_h^n} (\{\boldsymbol{n} \cdot \boldsymbol{\sigma}(\boldsymbol{u})\}, [\boldsymbol{w}_h])_e \Big| \\ &\leq C \Big| \sum_{e \in \varepsilon_h^n} (\boldsymbol{n} \cdot \boldsymbol{\sigma}(\boldsymbol{u}) - \overline{\boldsymbol{n} \cdot \boldsymbol{\sigma}(\boldsymbol{u})}, [\boldsymbol{w}_h])_e \Big| \\ &\leq Ch\|\boldsymbol{u}\|_{\widetilde{H}^2(\Omega)} \|\boldsymbol{w}_h\|_h. \end{aligned} \tag{4.45}$$

Furthermore, by Theorem 3.5,

$$\inf_{\forall \boldsymbol{v}_h \in S_{h,0}(\Omega)} \|\boldsymbol{u} - \boldsymbol{v}_h\|_h \leq Ch\|\boldsymbol{u}\|_{\widetilde{H}^2(\Omega)}. \tag{4.46}$$

Combining (4.44) with (4.45) and (4.46), the proof is completed. □

5. Numerical examples

In this section, some numerical examples are gived to show the performance of our partially penalized P_1/CR IFE method. Let $\Omega = (-1, 1) \times (-1, 1)$ be the solution domain. We denote the approximation error of the IFE interpolation by $\boldsymbol{u} - \boldsymbol{I}_h\boldsymbol{u}$ and the IFE solution error by $\boldsymbol{u} - \boldsymbol{u}_h$, which are measured in L^2 and the energy norm. In the following error tables, rates of convergence are computed by

$$\frac{1}{\log 2} \log \frac{\|\boldsymbol{u} - \boldsymbol{v}_{2h}\|}{\|\boldsymbol{u} - \boldsymbol{v}_h\|}.$$

for a specific norm $\|\cdot\|$, where $\boldsymbol{v}_h = \boldsymbol{I}_h\boldsymbol{u}$ or $\boldsymbol{v}_h = \boldsymbol{u}_h$.

Example 1. This elasticity interface problem that we text has a circular interface Γ with radius $r_0 = \frac{\pi}{8}$. The domain Ω is divided into two sub-domains

$$\Omega^+ = \{(x, y) : x^2 + y^2 > r_0^2\} \qquad \Omega^- = \{(x, y) : x^2 + y^2 < r_0^2\}.$$

The exact solution is

$$\boldsymbol{u}(x, y) = \begin{pmatrix} u_1(x, y) \\ u_2(x, y) \end{pmatrix} = \begin{cases} \begin{pmatrix} u_1^-(x, y) \\ u_2^-(x, y) \end{pmatrix} = \begin{pmatrix} \frac{1}{\lambda^-} r^{\alpha_1} \\ \frac{1}{\lambda^-} r^{\alpha_2} \end{pmatrix} & \text{in } \Omega^-, \\ \begin{pmatrix} u_1^+(x, y) \\ u_2^+(x, y) \end{pmatrix} = \begin{pmatrix} \frac{1}{\lambda^+} r^{\alpha_1} + \left(\frac{1}{\lambda^-} - \frac{1}{\lambda^+}\right) r_0^{\alpha_1} \\ \frac{1}{\lambda^+} r^{\alpha_2} + \left(\frac{1}{\lambda^-} - \frac{1}{\lambda^+}\right) r_0^{\alpha_2} \end{pmatrix} & \text{in } \Omega^+, \end{cases}$$

where $\alpha_1 = 5$, $\alpha_2 = 7$ and $r = \sqrt{x^2 + y^2}$.

We consider three different coefficient configurations in the following tables. The first one is small jump in the Lamé parameters, $(\lambda^+, \lambda^-) = (5, 1)$, $(\mu^+, \mu^-) = (10, 2)$. The second one is moderate jump case, $(\lambda^+, \lambda^-) = (100, 1)$, $(\mu^+, \mu^-) = (200, 2)$. In the two cases, the Poisson ratios in two sub-domains are $\nu^{\pm} = \frac{1}{6}$ so that the material is compressible. The IFE interpolation error and the IFE solution error are optimal in L^2 norm and the energy norm.

In Table 3, let $(\lambda^+, \lambda^-) = (20000, 10000)$, $(\mu^+, \mu^-) = (20, 10)$ and the Poisson ratios are $\nu^+ = \nu^- \approx 0.4995$, which is corresponding to nearly incompressible case. The IFE interpolation error and the IFE solution error are also optimal. Moreover, we can observe that no locking phenomenon happens although the material is nearly incompressible.

Table 1: The interpolation errors and the IFE solution errors with $\lambda^+ = 5$, $\lambda^- = 1$, $\mu^+ = 10$, $\mu^- = 2$, $\nu^+ = \nu^- = 1/6$.

$\frac{1}{h}$	$\|\boldsymbol{u} - \boldsymbol{I}_h\boldsymbol{u}\|_{L^2}$	order	$\|\boldsymbol{u} - \boldsymbol{I}_h\boldsymbol{u}\|_h$	order
8	6.48e-002		1.36e-000	
16	1.66e-002	1.967	6.99e-001	0.961
32	4.17e-003	1.991	3.53e-001	0.994
64	1.05e-003	1.998	1.77e-001	0.998
128	2.61e-004	1.999	8.87e-002	0.999
$\frac{1}{h}$	$\|\boldsymbol{u} - \boldsymbol{u}_h\|_{L^2}$	order	$\|\boldsymbol{u} - \boldsymbol{u}_h\|_h$	order
8	8.97e-002		1.66e-000	
16	2.41e-002	1.893	8.74e-001	0.931
32	6.24e-003	1.951	4.45e-001	0.979
64	1.58e-003	1.981	2.24e-001	0.994
128	3.97e-004	1.994	1.12e-001	0.997

Table 2: The interpolation errors and the IFE solution errors with $\lambda^+ = 100$, $\lambda^- = 1$, $\mu^+ = 200$, $\mu^- = 2$, $\nu^+ = \nu^- = 1/6$.

$\frac{1}{h}$	$\|\boldsymbol{u} - \boldsymbol{I}_h\boldsymbol{u}\|_{L^2}$	order	$\|\boldsymbol{u} - \boldsymbol{I}_h\boldsymbol{u}\|_h$	order
8	3.24e-001		6.67e-000	
16	8.29e-002	1.965	3.43e-000	0.960
32	2.08e-002	1.991	1.73e-000	0.992
64	5.22e-003	1.998	8.66e-001	0.999
128	1.31e-003	1.999	4.34e-001	1.000
$\frac{1}{h}$	$\|\boldsymbol{u} - \boldsymbol{u}_h\|_{L^2}$	order	$\|\boldsymbol{u} - \boldsymbol{u}_h\|_h$	order
8	4.40e-001		8.16e-000	
16	1.19e-001	1.887	4.26e-000	0.938
32	3.08e-002	1.950	2.17e-000	0.976
64	7.81e-003	1.980	1.09e-000	0.993
128	1.96e-003	1.993	5.47e-001	0.998

Table 3: The interpolation errors and the IFE solution errors with $\lambda^+ = 20000$, $\lambda^- = 10000$, $\mu^+ = 20$, $\mu^- = 10$, $\nu^+ = \nu^- \approx 0.4995$.

$\frac{1}{h}$	$\|\boldsymbol{u} - \boldsymbol{I}_h\boldsymbol{u}\|_{L^2}$	order	$\|\boldsymbol{u} - \boldsymbol{I}_h\boldsymbol{u}\|_h$	order
8	1.62e-005		3.28e-004	
16	4.15e-006	1.966	1.68e-004	0.970
32	1.04e-006	1.991	8.46e-005	0.992
64	2.61e-007	1.998	4.24e-005	0.999
128	6.53e-008	1.999	2.13e-006	0.999
$\frac{1}{h}$	$\|\boldsymbol{u} - \boldsymbol{u}_h\|_{L^2}$	order	$\|\boldsymbol{u} - \boldsymbol{u}_h\|_h$	order
8	6.35e-003		9.84e-002	
16	2.02e-003	1.652	5.45e-002	0.857
32	5.63e-004	1.845	2.84e-002	0.945
64	1.47e-004	1.934	1.45e-002	0.978
128	3.75e-005	1.975	7.30e-003	0.990

Table 4: The interpolation errors and the IFE solution errors with $x_0 = 0$ and $x_0 = \frac{\pi}{200}$. $\lambda^+ = 2$, $\lambda^- = 1$, $\mu^+ = 3$, $\mu^- = 2$ and then $\nu^+ = 1/5$, $\nu^- = 1/6$.

Interface	$\frac{1}{h}$	$\|\boldsymbol{u} - \boldsymbol{I}_h\boldsymbol{u}\|_{L^2}$	order	$\|\boldsymbol{u} - \boldsymbol{I}_h\boldsymbol{u}\|_h$	order
$x_0 = 0$	16	2.16e-003		9.76e-001	
	32	5.44e-004	1.997	4.90e-002	0.997
	64	1.36e-004	1.999	2.45e-002	0.999
	128	3.40e-005	2.000	1.23e-002	1.000
$x_0 = \frac{\pi}{200}$	16	2.19e-003		1.00e-001	
	32	5.51e-004	1.995	5.04e-002	0.997
	64	1.38e-004	1.999	2.53e-002	0.999
	128	3.44e-005	2.000	1.27e-002	1.000
Interface	$\frac{1}{h}$	$\|\boldsymbol{u} - \boldsymbol{u}_h\|_{L^2}$	order	$\|\boldsymbol{u} - \boldsymbol{u}_h\|_h$	order
$x_0 = 0$	16	3.37e-003		1.32e-001	
	32	8.61e-004	1.984	6.68e-002	0.990
	64	2.16e-004	1.992	3.36e-002	0.997
	128	5.42e-005	1.998	1.69e-002	0.999
$x_0 = \frac{\pi}{200}$	16	3.38e-003		1.32e-001	
	32	8.70e-004	1.964	6.71e-002	0.981
	64	2.21e-004	1.981	3.37e-002	0.996
	128	5.49e-005	2.006	1.69e-002	1.000

Example 2. The interface curve Γ is a vertical straight line $x = x_0$ that separates the solution domain Ω into sub-domains

$$\Omega^+ = \{(x, y)^t : x > x_0\} \qquad \Omega^- = \{(x, y)^t : x < x_0\}.$$

The exact solution is given by

$$\boldsymbol{u}(x,y)) = \begin{pmatrix} u_1(x,y) \\ u_2(x,y) \end{pmatrix} = \begin{cases} \begin{pmatrix} u_1^-(x,y) \\ u_2^-(x,y) \end{pmatrix} = \begin{pmatrix} \frac{1}{\lambda^-+2\mu^-}(x-x_0)\cos(2xy) \\ \frac{1}{\mu^-}(x-x_0)\cos(2xy) \end{pmatrix} & \text{in } \Omega^-, \\ \begin{pmatrix} u_1^+(x,y) \\ u_2^+(x,y) \end{pmatrix} = \begin{pmatrix} \frac{1}{\lambda^++2\mu^+}(x-x_0)\cos((x+x_0)y) \\ \frac{1}{\mu^+}(x-x_0)\cos((x+x_0)y) \end{pmatrix} & \text{in } \Omega^+. \end{cases}$$

In Table 4, let $(\lambda^+, \lambda^-) = (2,1)$, $(\mu^+, \mu^-) = (3,2)$ and $(\nu^+, \nu^-) = (\frac{1}{5}, \frac{1}{6})$. The interface location varies from $x_0 = 0$ to $x_0 = \frac{\pi}{200}$. The rates of convergence in L^2 norm and the energy norm confirm our error analysis.

Table 5: The interpolation errors and the IFE solution errors with $x_0 = 1 - \frac{\pi}{300}$, $\lambda^+ = 2$, $\lambda^- = 1$, $\mu^+ = 3$, $\mu^- = 2$, $\nu^+ = 0.2$, $\nu^- = 1/6$.

$\frac{1}{h}$	$\|\boldsymbol{u} - \boldsymbol{I}_h\boldsymbol{u}\|_{L^2}$	order	$\|\boldsymbol{u} - \boldsymbol{I}_h\boldsymbol{u}\|_h$	order
8	2.74e-003		7.41e-002	
16	6.93e-004	1.986	3.73e-002	0.991
32	1.74e-004	1.998	1.87e-002	0.997
64	4.34e-005	2.000	9.37e-003	0.999
128	1.09e-005	1.990	4.70e-003	0.998
$\frac{1}{h}$	$\|\boldsymbol{u} - \boldsymbol{u}_h\|_{L^2}$	order	$\|\boldsymbol{u} - \boldsymbol{u}_h\|_h$	order
8	5.23e-003		1.09e-001	
16	1.33e-003	1.981	5.48e-002	0.992
32	3.33e-004	1.992	2.75e-002	0.996
64	8.37e-005	1.994	1.38e-002	0.999
128	2.10e-005	1.997	6.94e-003	0.998

Table 6: The interpolation errors and the IFE solution errors with $x_0 = 1 - \frac{\pi}{300}$, $\lambda^+ = 2000$, $\lambda^- = 1000$, $\mu^+ = 3$, $\mu^- = 1$, $\nu^+ \approx 0.4995$, $\nu^- \approx 0.4993$.

$\frac{1}{h}$	$\|\boldsymbol{u} - \boldsymbol{I}_h\boldsymbol{u}\|_{L^2}$	order	$\|\boldsymbol{u} - \boldsymbol{I}_h\boldsymbol{u}\|_h$	order
8	1.89e-003		9.12e-002	
16	4.80e-004	1.973	4.58e-002	0.995
32	1.21e-004	1.985	2.30e-002	1.001
64	3.05e-005	1.990	1.16e-002	0.997
128	7.95e-006	1.942	5.84e-003	0.992
$\frac{1}{h}$	$\|\boldsymbol{u} - \boldsymbol{u}_h\|_{L^2}$	order	$\|\boldsymbol{u} - \boldsymbol{u}_h\|_h$	order
8	8.17e-001		1.36e+001	
16	2.04e-001	2.000	6.82e-000	1.003
32	5.11e-002	2.000	3.42e-000	1.000
64	1.28e-002	2.001	1.71e-000	0.999
128	3.19e-003	2.000	8.58e-001	1.000

In Tables 5 and 6, we put the interface $x_0 = 1 - \frac{\pi}{300}$ near the left boundary. Let the Lamé coefficients are $(\mu^+, \mu^-) = (3,2)$, $(\lambda^+, \lambda^-) = (2,1)$, and $(\mu^+, \mu^-) = (3,1)$,

$(\lambda^+, \lambda^-) = (2000, 1000)$, respectively. The numerical results show that the IFE interpolation error and the IFE solution error orders in L^2 norm and the energy norm are optimal.

Example 3. Ω is separated by an ellipse interface curve Γ into subdomains $\Omega^+ = \{(x,y)^t : x^2 + 4y^2 > r_0^2\}$ and $\Omega^- = \{(x,y)^t : x^2 + 4y^2 < r_0^2\}$. Let $r_0 = 0.2$, the exact solution is

$$\boldsymbol{u}(x,y)) = \begin{pmatrix} u_1(x,y) \\ u_2(x,y) \end{pmatrix} = \begin{cases} \begin{pmatrix} u_1^-(x,y) \\ u_2^-(x,y) \end{pmatrix} = \begin{pmatrix} \frac{1}{\lambda^- + 2\mu^-}\left(x^2 + 4y^2 - r_0^2\right) \\ \frac{1}{\mu^-}\left(x^2 + 4y^2 - r_0^2\right) \end{pmatrix} & \text{in } \Omega^-, \\ \begin{pmatrix} u_1^+(x,y) \\ u_2^+(x,y) \end{pmatrix} = \begin{pmatrix} \frac{1}{\lambda^+ + 2\mu^+}\left(x^2 + 4y^2 - r_0^2\right) \\ \frac{1}{\mu^+}\left(x^2 + 4y^2 - r_0^2\right) \end{pmatrix} & \text{in } \Omega^+. \end{cases}$$

Table 7: The interpolation errors and the IFE solution errors with $\lambda^+ = 100$, $\lambda^- = 1$, $\mu^+ = 200$, $\mu^- = 2$.

$\frac{1}{h}$	$\|\boldsymbol{u} - \boldsymbol{I}_h\boldsymbol{u}\|_{L^2}$	order	$\|\boldsymbol{u} - \boldsymbol{I}_h\boldsymbol{u}\|_h$	order
8	2.93e-002		6.34e-001	
16	7.40e-003	1.985	3.22e-001	0.983
32	1.85e-003	1.999	1.61e-001	1.000
64	4.63e-004	1.998	8.08e-002	0.999
128	1.16e-004	1.999	4.05e-002	1.000
$\frac{1}{h}$	$\|\boldsymbol{u} - \boldsymbol{u}_h\|_{L^2}$	order	$\|\boldsymbol{u} - \boldsymbol{u}_h\|_h$	order
8	6.30e-002		1.10e-000	
16	1.65e-002	1.933	5.57e-001	0.984
32	4.43e-003	1.897	2.81e-001	0.989
64	1.12e-003	1.978	1.41e-001	1.000
128	2.79e-004	2.012	7.05e-002	1.000

Table 8: The interpolation errors and the IFE solution errors with $\lambda^+ = 20000$, $\lambda^- = 10000$, $\mu^+ = 20$, $\mu^- = 10$, $\nu^+ = \nu^- \approx 0.4995$.

$\frac{1}{h}$	$\|\boldsymbol{u} - \boldsymbol{I}_h\boldsymbol{u}\|_{L^2}$	order	$\|\boldsymbol{u} - \boldsymbol{I}_h\boldsymbol{u}\|_h$	order
8	2.15e-003		6.71e-002	
16	5.27e-004	2.027	3.38e-002	0.993
32	1.31e-004	2.005	1.69e-002	1.002
64	3.27e-005	2.006	8.49e-003	1.000
128	8.16e-006	2.002	4.26e-003	0.999
$\frac{1}{h}$	$\|\boldsymbol{u} - \boldsymbol{u}_h\|_{L^2}$	order	$\|\boldsymbol{u} - \boldsymbol{u}_h\|_h$	order
8	2.71e-000		3.87e+001	
16	7.31e-001	1.890	1.99e+001	0.956
32	1.87e-001	1.969	1.00e+001	0.990
64	4.77e-002	1.970	5.05e-000	0.989
128	1.22e-002	1.967	2.56e-000	0.986

Table 7 presents the numerical results for the case $(\lambda^+, \lambda^-) = (100, 1)$, $(\mu^+, \mu^-) = (200, 2)$. We text nearly incompressible case in Table 8, where $(\lambda^+, \lambda^-) = (20000, 10000)$, $(\mu^+, \mu^-) = (20, 10)$, the Poisson ratios in sub-domains are $\nu^+ = \nu^- \approx 0.4995$. The numerical results indicate that the convergence orders of the P_1/CR IFE method in L^2 norm and the energy norm are optimal, no matter the material is compressible or almost incompressible.

In conclusion, ~~we develop~~ a partially penalized IFE method for solving elasticity interface problems on triangular unfitted-meshes and give the optimal error estimate of the IFE solution. The numerical results also confirm the rate of convergence is optimal in L^2 norm and the energy norm.

References

[1] S. Adjerid, T. Lin and J. Wang. *Higher-order immersed discontinuous Galerkin methods.* Int. J. Inf. Syst. Sci., 3 (2007), 555-568.

[2] D. N. Arnold. *An interior penalty finite element method with discontinuous elements.* SIAM J. Numer. Anal., 19 (1982), 742-760.

[3] I. Baluška. *The finite element method for elliptic equations with discontinuous coefficients.* Computing, 5 (1970), 207-213.

[4] I. Baluška. *Locking effect in the finite element approximation of elasticity problem.* Numer. Math. 62, (1992), 439-463.

[5] P. Bastin and C. Engwer. *An unfitted finite element method using discontinuous Galerkin.* Internat. J. Numer. Methods Engrg., 79 (2009), 1557C1576.

[6] J. Barrett and C. Elliott. *Fitted and unfitted finite-element methods for ellipticequations with smooth interfaces.* IMA J. Numer. Anal., 7 (1987), 283C300.

[7] S. C. Brenner, and L. Y. Sung. *Linear finite element methods for planar linear elasticity.* Math. Comp, 59, (1992), 321-338.

[8] F. Brezzi, and M. Fortin. *Mixed and hybrid finite element methods.* Springer-Verlag, New-York, 1991.

[9] Z. Chen and J. Zou. *Finite element methods and their convergence for elliptic and parabolic interface problems.* Numer. Math., 79 (1998), 175-202.

[10] M. Crouzeix and P. A. Raviant. *Conforming and nonconforming finite element methods for solving the stationary Stokes equations.* RARIO. Anal. Numér, 7.R3 (1973), 33-75.

[11] J. Doulbow, N. Moës and T. Belystischko. *Interior penalty procedures for elliptic and parabolic Galerkin methods.* Computing Methods in Applied Sciences, Lecture Notes in Phys. Springer, Berlin, 58 (1976), 207-216.

[12] R. S. Falk. *Nonconforming finite element methods for the equations of linear elasticity.* Mathematics of Computation, 57 (1991), 529-550

[13] Y. Gong, B. Li and Z. Li. *Immersed-interface finite element methods for elliptic interface problems with nonhomogeneous jump conditions.* SIAM J. Numer. Anal., 46 (2008), 472-495.

[14] H. Gao, y. Huang and F.F. Abraham. *Continuum and atcmistic studies of intersonic crack propagation.* I.Mech. Phys. Solids, 49 (2001), 2113-2132.

[15] Y. Gong and Z. Li. *Immersed interface finite element methods for elasticity interface problems with non-homogeneous jump conditions.* Numer. Math. Theory Methods Appl., 3 (2010), 23-39.

[16] A. Hansbo and P. Hansbo. *An unfitted finite element method, based on Nitsche's method, for elliptic interface problems.* Comput. Methods Appl. Mech. Engrg., 191 (2002), 5537-5552.

[17] P. Hansbo and M. G. Larson. *Discontinuous Galerkin and the Crouzeix-Raviart element: Applications to elasticity.* Mathematical Modelling and Numerical Analysis, ESAIM, Vol. 37 (2003), 63-72.

[18] A. Hansbo and P. Hansbo. *A finite element method for the simulation of strong and weak discontinuities in solid mechanics.* Comput. Methods and Numer. Mech. Engrg., 193 (2004), 3523-3540.

[19] X. He, T. Lin and Y. Lin. *Approximation capability of a bilinear immersed finite element space.* Numer. Methods Partial Differetial Equations, 24 (2008), 1265-1300.

[20] X. He, T. Lin and X. Zhang. *Immersed finite element methods for parabolic equations with moving interface.* Numer. Methods Partial Differetial Equations, 29 (2013), 619-646.

[21] R. Kafafy, T. Lin and J. Wang. *Three-dimensional immersed finite element methods for electric field simulation in composite materials.* Internat. J. Numer. Methods. Engrg., 64 (2005), 940-972.
[22] R. Kouhia, R. Stenberg. *A linear nonconforming finite element method for nearly incompressible elasticitu and stokes flow.* Comput. Methods Appl. Mech. Engrg., 124 (1995), 195-212.
[23] D. Y. Kwak, K. T. Wee and K. S. Chang. *An analysis of a broken P_1-nonconforimng finite element method for interface problems.* SIAM J. Numer. Anal., 48 (2010), 2117-2134.
[24] A. Liu, J. Chen. *A partially penalized P1/CR immersed finite element method for planar elasticity interface problem.* Numerical Methods for Partial Differential Equations, (2019), 2318-2347.
[25] Z. Li. *The immersed interface method using a finite element formulation.* Appl. Numer. Math., 27 (1998), 253-267.
[26] Z. Li, T. Lin Y. Liu, and R. C. Rogers. *An immersed finite element space and its approximation capability.* Numerical Methods for Partial Differential Equations, 20 (2004), 338-367.
[27] Z. Li, T. Lin and X. Wu. *New Cartesian grid methods for interface problem using the finite element formulation.* Numer. Math., 96 (2003), 61-98.
[28] T. Lin, Y. Lin and X. Zhang. *Partially penalized immersed finite element methods for elliptic interface problems.* SIAM J. Numer. Anal., 53 (2015), 1121-1144.
[29] T. Lin and D. Sheen. *The immersed finite element method for parabolic problems with the Laplace transformation in time discretization.* Int. J. Numer. Anal. Model., 10 (2013), 298-313.
[30] T. Lin, D. Sheen and X. Zhang. *A locking-free immersed finite element method for planar elasticity interface problems.* J. Comput. Appl. Math., 236 (2012), 4681-4699.
[31] T. Lin, D. Sheen and X. Zhang. *Nonconforming immersed finite element methods for elliptic interface problems.* arXiv preprint arXiv:1510.00052, 2015.
[32] Z. Li and X. Yang. *An Immersed interface finite element methods for elasticity equations with interfaces.* Contemporary Mathematics, 383 (2005), 285-298.
[33] F. Qin, J. Chen, Z. Li, M. Cai. *A Cartesian grid nonconforming immersed finite element method for planar elasticity interface problems.* Computers and Mathematics with Applications, 73 (2017), 404-418.
[34] T. Lin and X. Zhang. *Linear and bilinear immersed finite elements for planar elasticcity interface problems.* J. Comput. Appl. Math., 236 (2012), 4681-4699.
[35] A. Reusken. *Analysis of an extended pressure finite element space for two-phase incompressible flows.* Comput. Vis. Sci., 11 (2008), 293-305.
[36] A. Reusken and T. Nguyen. *Nitsche's method for a transport problem in two-phase incompressible flows.* J. Fourier. Anal. Appl., 15 (2009), 663-683.
[37] A. Sutton and R. Balluffi. *Interfaces in Crystalline Materials.* Clarendor Press, 1995.
[38] C.-T. Wu, Z. Li and M.-C. Lai. *Adaptive mesh refinement for elliptic interface problems using the non-conforming immersed finite element method .* Int. J. Numer. Anal., 8 (2011), 466-483.
[39] X. Zhang. *Nonconforming immersed finite element methods for interface problems.* Thesis (Ph.D.)-Virginia Polytechnic Institute and State University, (2013).